Self-excited void instability in dusty plasmas: plasma and dust cloud dynamics during the heartbeat instability

Maxime Mikikian, Lénaïc Couëdel, Marjorie Cavarroc, Yves Tessier, Laifa Boufendi

New Journal of Physics
The open-access journal for physics

Self-excited void instability in dusty plasmas: plasma and dust cloud dynamics during the heartbeat instability

M Mikikian, L Couëdel, M Cavarroc, Y Tessier and L Boufendi

GREMI, Groupe de Recherches sur l'Energétique des Milieux Ionisés, UMR6606, CNRS/Université d'Orléans, 14 rue d'Issoudun, BP6744, 45067 Orléans Cedex 2, France
E-mail: maxime.mikikian@univ-orleans.fr

New Journal of Physics **9** (2007) 268
Received 30 March 2007
Published 15 August 2007
Online at http://www.njp.org/
doi:10.1088/1367-2630/9/8/268

Abstract. When a three-dimensional dust cloud is present in a plasma, a dust-free region, called a void, is usually obtained in the plasma centre. Under certain conditions, this region exhibits a self-excited unstable behaviour consisting of successive contractions and expansions of its size. In this paper, this low frequency instability (few Hz), called a 'heartbeat', is characterised by various diagnostics. Electrical and optical measurements both correlated with high speed imaging brought to the fore the main features of this instability. Forces involved in the void existence are an inward electrostatic force and an outward ion drag one. The force balance ensures an open void but this equilibrium can be disturbed, leading to the observed instabilities. As these forces are strongly dependent on local ionisation conditions, correlations between physical processes in the plasma volume and the dust cloud motion are investigated through experimental results.

PII: S1367-2630(07)47353-0

Contents

1. Introduction

Dusty plasmas are relatively complex systems where new phenomena arise from the presence of solid dust particles trapped inside the plasma. Usually, this trapping is a consequence of the negative charge acquired by the dust particles [1]–[6] immersed in a medium partly composed of free electrons. The full dust particle dynamics is then described by charge dependent forces (mainly electric and ion drag forces) and other ones like gravity, neutral drag and thermophoresis. Relative amplitudes of these forces are strongly dependent on the dust particle size. In the micrometre range, dust particles are usually directly injected in the plasma volume. Their weight is non-negligible and some phenomena are only observed under microgravity conditions [7, 8]. Nevertheless, their big size allows an easy and precise visualisation in laboratory experiments. In the submicrometre range, dust particles are usually grown in the plasma using methods based on reactive gases or material sputtering.

Reactive gases are used due to their ability to form dust particles by following a rather complicated succession of growth phases. One of the most studied and well-known reactive gas is silane (SiH_4) [9]–[15]. The interest for silane based chemistry is mainly due to its implication in microelectronics and/or nanotechnology. Indeed, in the late 1980s, dust particle formation in the gas phase has been evidenced in reactors used for silicon based device fabrication [9, 16]. In some processes, cleanliness is a major requirement and a lot of studies began for understanding dust particle formation and growth in order to avoid their deposition. More recently, silicon nanocrystal formation [17] became of high interest for their incorporation in thin films in order to improve their properties. Indeed, their use in solar cell technology enhances optoelectronic properties of deposited films [18]. Single electron devices (SED) like transistors [19] or memories [20] can also be built, thanks to these silicon nanocrystals. Dust particle formation in hydrocarbon based gases like methane (CH_4) [21]–[23] or acetylene (C_2H_2) [21, 22, 24, 25] has also been studied. Indeed, CH_4 and C_2H_2 are used for deposition

of diamond-like carbon (DLC) films [26] or nanocrystalline diamond [27] used in industry for their unique properties like extreme hardness. Hydrocarbon gases are also of great interest for the astrophysical community dealing with planet atmospheres like Titan, where dust particles are created from a mixture of methane and nitrogen [28].

Another process for dust particle production is material sputtering [29]–[32]. This phenomenon can appear in industrial reactors and also in fusion devices [33] like Tore Supra [34] where graphite walls can be severely eroded by ion bombardment. Produced dust particles can strongly limit performances of the fusion plasma. This aspect is of great importance for the future ITER reactor.

Dust particles levitating in the full plasma volume can be obtained under microgravity (for micrometre dust particles) or in the laboratory (for submicrometre dust particles). Usually, the three-dimensional dust cloud exhibits a specific feature consisting of a centred egg-shaped region free of dust particles. This region, called a 'void' [7, 31, 32], [35]–[47], seems to be controlled by an equilibrium between the charge dependent forces (inward electrostatic and outward ion drag forces). This stable state is sometimes disturbed and void size oscillation can occur. This self-excited instability is named the 'heartbeat' instability [36, 46, 48, 49]. It has been previously observed during microgravity experiments with injected micrometre dust particles and has since also been studied in the laboratory with grown submicrometre dust particles [49]–[52]. In these last experiments, investigations of the heartbeat instability have been performed using both electrical and spatially resolved optical diagnostics. These measurements allowed to identify complex behaviours in recorded signals roughly related to dust particle motion. Furthermore, the threshold behaviour of this self-excited instability has been brought to the fore [51, 52]. Nevertheless, the presence of a sharp peak in electrical measurements and its absence in optical ones was still unclear. Further investigations have been conducted using high speed imaging to record dust particle cloud motion. These preliminary results gave first insights concerning dust cloud motion and void size evolution correlated with electrical signals [51, 52]. In the present paper, new results on the heartbeat instability are obtained thanks to a second high speed imaging experiment. Behaviour of both dust cloud and plasma glow is investigated and correlations between both types of data are deduced. These results are compared to electrical measurements and previous spatially resolved optical ones. The void dynamics during the instability is now better characterised and, for example, the sharp peak presence can be correlated with plasma glow changes.

2. Experimental set-up

2.1. Reactor

Experiments are performed in the Plasma Kristall Experiment (PKE)-Nefedov chamber [8, 32]. The plasma is produced by a capacitively coupled radio frequency (rf) discharge operating in push–pull mode at 13.56 MHz. The planar parallel electrodes are 4 cm in diameter and are separated by 3 cm. In this chamber, argon is introduced to a typical pressure of 1.6 mbar and the plasma is ignited with a rf power of typically 2.8 W. Dust particles are grown by sputtering a polymer layer deposited on the electrodes and constituted of previously injected melamine formaldehyde dust particles.

2.2. Diagnostics

Grown dust particles are observed by laser light scattering using a thin laser sheet produced by a laser diode at 685 nm and three standard charge coupled device (CCD) cameras (25 frames per second) equipped with narrow-bandwidth interference filters. Two of these cameras record the scattered light at 90° with different magnifications. The third one looks at the cloud with an angle lying approximately between 20° and 30° with respect to the incident laser direction. This camera allows the observation of grown dust particles when their size is too small to observe them at 90°.

Plasma and dust particle cloud behaviours are strongly linked and a modification in one of these media is usually reflected in the other. Therefore, diagnostics able to analyse both systems are used in order to better characterise the heartbeat instability.

The first one consists of the measurement of the time evolution of the amplitude of the discharge current fundamental harmonic. Indeed, this diagnostics is representative of global changes in plasma properties and can be related to electron density variations. It allows to monitor the total current during the various phases of the instability very easily. Thus, it is used as our reference diagnostics. It shows that the heartbeat instability has different signatures depending on the pressure, power and dust particle density [49].

The second diagnostics is based on spatially resolved optical measurements performed in two different ways. The time evolution of either the intensity of an argon line or the total plasma light is recorded in different plasma regions. For the total plasma light recording, five optical fibres are horizontally aligned (separated by 5 mm) with a spatial resolution of about 3 mm. This diagnostic is complementary to the electrical one because it can detect any plasma motion or local behaviours that cannot be evidenced by a global measurement.

The third diagnostics consists of high speed imaging. The observed instability oscillates at relatively low frequencies (10–200 Hz) but too high to be finely characterised by standard CCD cameras at 25 frames per second. Indeed, as previously observed [49], some features of the instability, like the sharp peak, take place during a typical time scale of about 1 ms. A high speed video camera system with 1789 frames per second (Mikrotron MC 1310) is used to observe either the plasma glow or the dust cloud. Thus, two successive frames are separated by around 560 μs. For the last observation, the high speed camera takes the place of the third standard CCD camera in order to record more light scattered by the dust cloud.

As already mentioned, the heartbeat instability has different signatures and measurements show a wide variety of frequencies and shapes. In the following sections, both dust cloud and plasma glow will be analysed in two different cases considered as sufficiently different to cover a wide range of experimental observations: a low repetition rate one (contraction–expansion sequences are well separated and original conditions, i.e. stable void, are nearly restored between each sequence) and a high repetition rate one (continuous motion of the void). The high repetition rate occurs when the instability is well established (higher values of injected rf power) whereas low repetition rate occurs at lower powers when the instability tends to slow down before stopping. Plasma glow will be mainly discussed through its intensity (thus ‘glow intensity’ is referred as ‘glow’ in the following), except when spatial concerns are well specified. Following results will mainly concern the fully developed instability. Another interesting phenomenon, consisting of failed contractions [51, 52] appearing near the instability existence threshold, will be analysed in a further article.

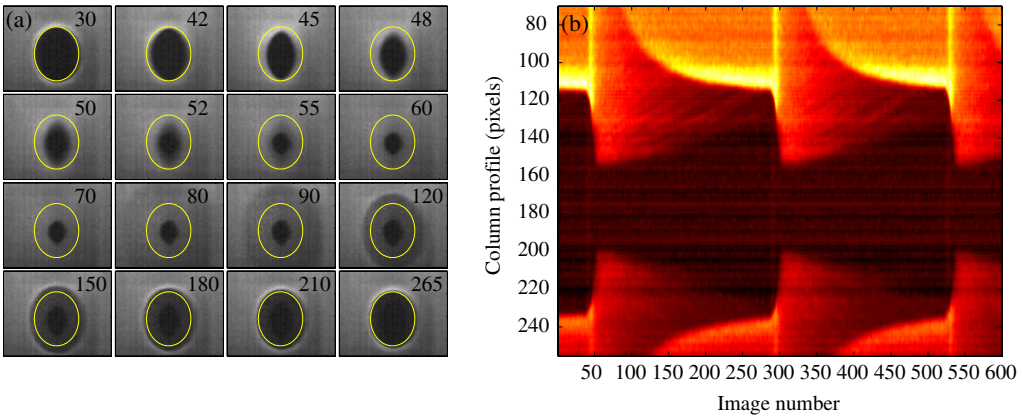

Figure 1. Heartbeat instability for a low repetition rate observed on the dust cloud. (a) Some images of the void region during one contraction–expansion sequence. The yellow ellipse delineates position of the stable open void. (b) Time evolution of central column profile (vertical line passing through the void centre) constructed from the entire video in false colours (from dark red to bright yellow) (see also movie 1, 3.9 MB MPEG).

3. Dust cloud and plasma glow behaviours near the void region

In order to characterise the heartbeat instability, a first approach consists of a direct visualisation of the void with its surrounding dust cloud. Typical unstable voids have a size of about a few millimetres. Beyond a certain size, voids are usually stable and no instability has been observed in the explored parameter range. Indeed, in this case, their stability is not disturbed even by decreasing the pressure or increasing the power (these changes are known to be able to initiate the heartbeat instability [49]).

3.1. Sequences with a low repetition rate

A video corresponding to a low repetition rate and showing three successive contraction–expansion sequences is available in figure 1. Some extracted images from the first sequence are shown in figure 1(a). Image aspect ratio is distorted due to the view angle compressing the horizontal direction. Image numbers appear on the top right part of each image. The drawn ellipse represents the position of the stable open void determined from image 30. Small but detectable motion starts at image 40 (not shown) and clearly appears at image 42 where dust cloud boundaries are clearly inside the drawn ellipse. Contraction lasts up to image 55 where the void reaches its minimum size. From this instant, the empty inner part slowly increases in size while a light grey corona region (i.e. lower dust density region) starts to be detected in image 80 and slowly reduces in size. These two regions meet and the stable open void state is nearly reached anew in image 265.

In order to better depict this contraction–expansion sequence, the time evolution of a column profile is shown in figure 1(b). To construct this false colour image, the vertical line passing through the void centre is extracted from each video image. Time is represented by image number in the x-axis and column profile is given in the y-axis. Using the video as a reference, this representation is of interest in that it gives in one single image a clear

characterisation of the instability in both time and space. Low dust density regions appear dark while high dust density ones appear bright. Three contractions and two expansions are clearly evidenced and give a frequency of about 7 Hz. For the first sequence, images 1–40 show the higher dust density region usually observed in the void boundaries. Then, the contraction takes place and the void reaches its minimum size approximately 2.5 times smaller than the stable void size. At this moment, the two previously described phenomena (size increase of the dark inner part and size decrease of an intermediate grey corona region) are well resolved in time. The regular size increase of the inner part can be directly correlated to the void size increase assuming that the term 'void' stands for the null dust density region. From figure 1, the behaviour of the corona region seems to correspond to the motion of dust particles attracted to the plasma centre during the contraction and going back to their original stable position. This motion is characterised by a moving boundary between a region of high dust density and another one of low dust density. It appears that the speed of this moving boundary decreases as it approaches the original void position. The dust particles which are the closest to the centre, react last with the smallest speed. Furthermore, the corona region in its maximum extension is larger than the size of the stable void indicating that the instability affects the dust cloud over a long distance and not only in the close vicinity of the void. Collective motions can take place on long distances due to the strong interaction between dust particles and their strong coupling with plasma changes. Finally, figure 1(b) shows that inner and corona regions meet (around image 280) and the high dust density boundaries are restored just before another contraction occurs.

To complete these observations, the interference filter is removed from the high speed camera in order to record plasma glow evolution without changing the camera position. The obtained image series is acquired approximately 2 s after the one presented in figure 1, checking that the instability does not change neither in frequency nor in shape. In order to synchronise dust cloud images with plasma glow ones, small residual plasma glow signal passing through interference filter is used (slightly visible in figure 1(b) in the black inner part of the void but not allowing analysis). Electrical measurements are used to check that instability characteristics remain unchanged. Typical images are presented in figure 2(a). In order to bring out changes, a reference image is subtracted and false colours are used. Plasma glow images shown in figure 2(a) correspond to the dust cloud ones shown in figure 1(a). For comparison, the same ellipse as in figure 1(a) is superimposed on the glow images. By correlating both dust cloud and glow images, it clearly appears that the void contraction seems to correspond to a glow enhancement in the plasma centre. Intermediate images of the glow variation are shown in figure 2(b). It appears that the concerned plasma region is bigger than the original void region even if maximum glow values are inside the void. This aspect can explain why the light grey corona region observed in figure 1 has a maximum extension bigger than the stable void. In fact, the first image showing the glow increase is image 10 in figure 2(b), where the bright region is already bigger than the drawn ellipse. Due to camera speed limitation, some data are missing between images 9 and 10. Consequently it cannot be concluded if, at the early beginning, the enhancement is bounded by the void and then propagates, or if it concerns directly a bigger size region. After reaching its maximum value (around image 13), plasma glow decreases and reaches a minimum below the mean glow value (darker image 19 in figure 2(a)). Certainly due to dust particle inertia, the void continues to shrink (figure 1(a)) but when the central glow (i.e. ionisation and consequently ion drag force) starts to increase slowly (from image 26 in figure 2(a) corresponding to image 55 in figure 1(a)), the contraction stops and expansion occurs.

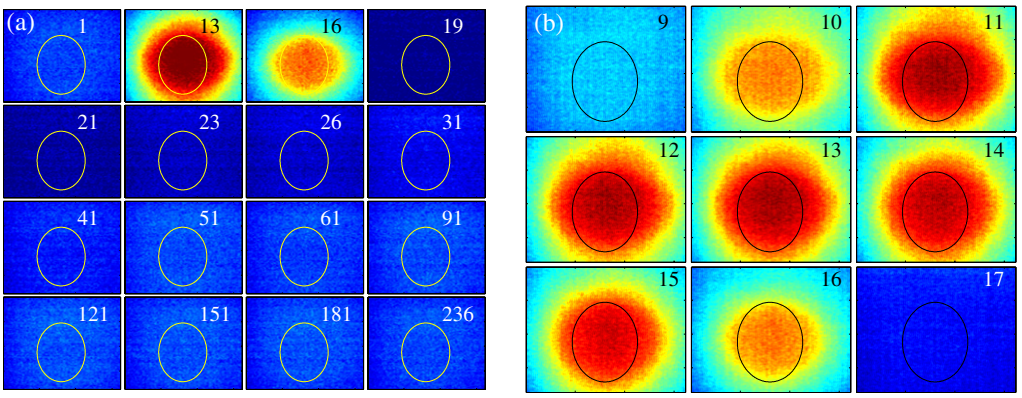

Figure 2. Heartbeat instability for a low repetition rate observed on the plasma glow. (a) Some images of the void region (in false colours from dark blue to red) during one contraction–expansion sequence (image 1 corresponds to image 30 of figure 1 and so on). The yellow ellipse delineates position of the stable open void. (b) Intermediate images of (a) during fast plasma glow modifications.

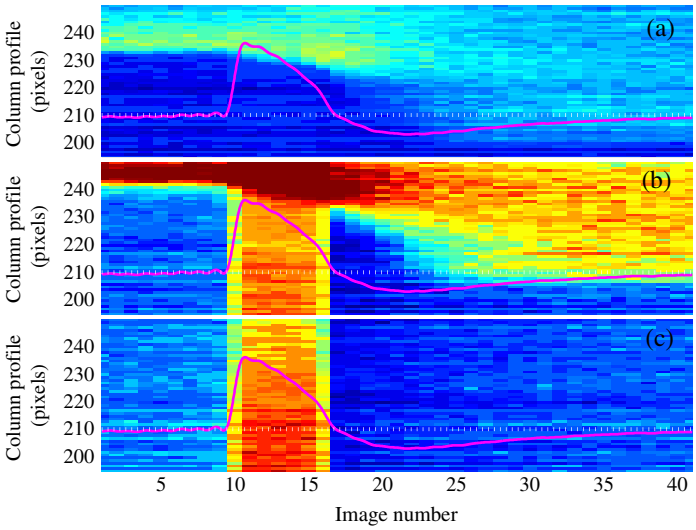

Figure 3. Heartbeat instability for a low repetition rate: electrical measurements superimposed on column profiles from (a) only dust cloud; (b) dust cloud and plasma glow, (c) only plasma glow. Parts (a), (b) and (c) in false colours (from dark blue to red).

Column profiles of these different series can be compared. Figure 3 shows synchronised profiles obtained from videos showing (a) the dust cloud (laser and camera with interference filter), (b) dust cloud and glow (laser and camera without interference filter) and (c) plasma glow (neither laser nor interference filter). Electrical measurements are superimposed with their mean value (dotted line) corresponding to the stable open void. In figure 3(c) it appears that there is a good correlation between plasma glow and electrical measurements as the main variations are related. The fast signal increase corresponds to glow enhancement. It is followed by a decrease in both sets of data. A small shoulder appearing in electrical measurements (slope change) is

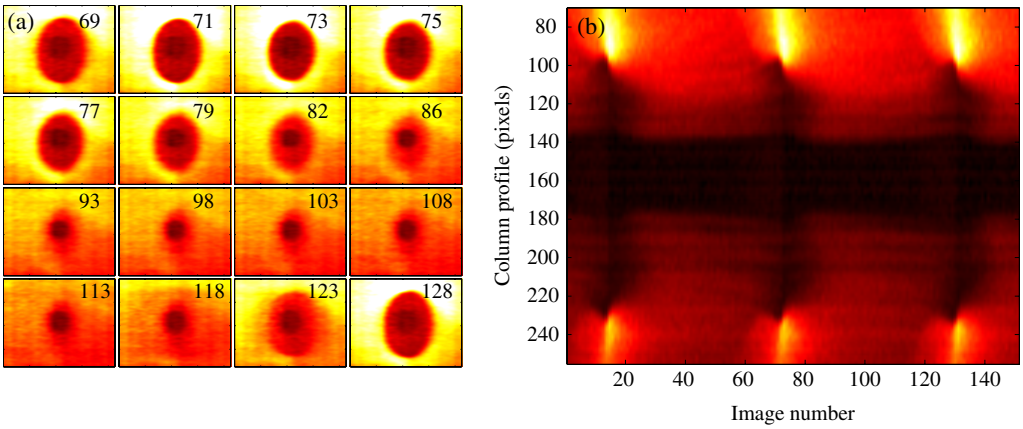

Figure 4. Heartbeat instability for a high repetition rate observed on the dust cloud: (a) some images of the void region (in false colours from dark red to bright yellow) during one contraction–expansion sequence; (b) time evolution of central column profile constructed from the entire video (see also movie 2, 2.3 MB).

related to a more drastic decrease of the central plasma glow. Then, the following minimum values of both data are close in time. After this point, the next plasma glow increase towards the mean state is well observed in electrical measurements slowly tending towards the mean value. As mentioned, global variations are similar but some discrepancies exist due to the fact that electrical measurements are integrated on all the plasma volume, and contain information on plasma variation occurring outside the plasma centre. This aspect will be explored in section 4, where a precise analysis of the entire plasma glow is performed. Concerning the dust cloud, the void contraction is related to glow and electrical signal increase (figures 3(a) and (b)), meaning that it corresponds to ionisation increase in the plasma centre. Nevertheless, it can be observed that contraction continues even when the electrical signal starts decreasing and is still not stopped when electrical measurements and plasma glow are below their original value. It confirms the direct comparison between dust cloud and plasma glow performed through figures 1 and 2.

3.2. Sequences with a high repetition rate

Analysis of a high repetition rate sequence is more fussy due to the fast and constant motion of the dust cloud without any clear stable position giving a fixed reference. A movie is available in figure 4 and in the same way as in the low repetition rate case, extracted images and column profile are given respectively in figure 4(a) and (b). In order to increase contrast, false colours are also used for extracted images. The constant motion clearly appears: no horizontal bright regions, corresponding to high dust density void boundaries, are observed in figure 4(b). This figure gives a frequency instability of about 31 Hz. Furthermore, the inner part of the void region, which is never filled with dust particles, exhibits only small variations. Indeed, all the motion takes place in the low dust density region between the dense dust cloud and the void inner part. From the nearly isolated case (figure 1), this region has been identified to consist of dust particles going back to their original position. In the high repetition rate case, the new

contraction occurs while dust particles from the previous contraction are still inside the void and try to reach their original position. Indeed, a new contraction starts around image 69 of figure 4(a) (complex motions do not allow precise determination) while dust particles are still inside the void region. At this time the plasma glow is close to its maximum value in the centre (determined from a plasma glow video correlated to the present one). This complex behaviour leads to the relatively constant regions (black inner part and grey intermediate part) observed in figure 4(b). The dust cloud is always moving even so spatial dust density appears more or less constant.

3.3. Asymmetry in void contraction

Another interesting phenomenon concerning dust cloud motion during the heartbeat instability, is the observable delay appearing in the response of horizontal and vertical directions. Indeed, in some conditions (currently not clearly defined) the dust cloud shrinks horizontally before shrinking vertically [51, 52]. As an example, a record containing both dust cloud and plasma glow information has been performed for a sequence where a stable open void suddenly starts a size oscillation. First and second contraction–expansion sequences are shown in figure 5 where a movie can also be found. Image 135 clearly shows the stable open void with the corresponding drawn ellipse. In image 142 plasma glow starts increasing and reaches its maximum value at 144. In this last image, it appears that the plasma glow enhancement affects a region bigger than the void size and correlation with the corona region well observed in figure 1 can be suggested again. This hypothesis is correct assuming that the intensity increase in the surrounding dust cloud is entirely due to plasma glow changes and not due to any dust density modification. Thanks to the drawn ellipse, it clearly appears that the void shrinks first in the horizontal direction (starting from image 143) and then in the vertical one (starting around image 147). As images are already compressed in the horizontal direction, a detectable motion in this direction clearly indicates a real dust cloud response and cannot be an optical illusion. The plasma glow reaches its minimum value in image 148 and, as already observed, the void continues to shrink to its minimum size in image 155. From this point, the void inner part slowly increases in size and the grey intermediate region, constituted of dust particles going back to their original position, becomes gradually visible. The next contraction occurs before the original state has been completely reached again (image 241).

These various steps are well observed on the column profile shown in figure 6(a). For better understanding, temporal evolution of plasma glow in the central pixel of the void is superimposed at the bottom of the image. The stable open void is accurately defined with its constant size and its high dust density boundaries (between images 100 and 142). When plasma glow increases, the void shrinks. Its minimum size is reached while plasma glow in the centre has already reached its minimum value and has started to slowly increase again. Then, the glow stays relatively constant in the void centre while dust particles are expelled to their original position. It clearly appears that the void did not reach its original size when the new glow increase occurs. This effect is traduced, firstly by the dark inner part which does not rejoin the position of the stable void and secondly by the intermediate corona region which is bigger than the original void size. This last point means that the ‘wave front’ formed by returning dust particles is still moving towards the original void boundaries. The speed of this wave front appears to slow down when approaching the original conditions. Furthermore, it is clearly visible that the instability is in a setting up phase. Indeed, starting from a stable open void,

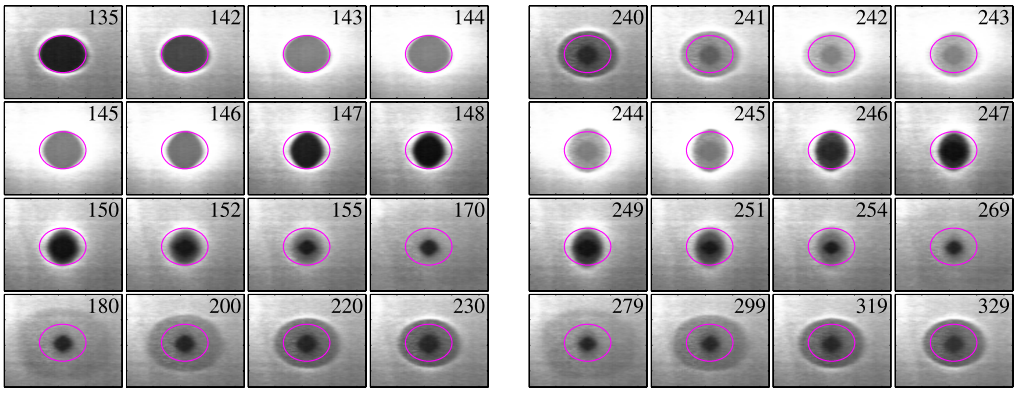

Figure 5. Simultaneous record of dust cloud and plasma glow in the void region during the setting up of the heartbeat instability. From image 135: stable open void (delineated by a pink ellipse) followed by a first contraction, and new contraction at image 241 while original conditions are not restored (see also movie 3, 2.6 MB).

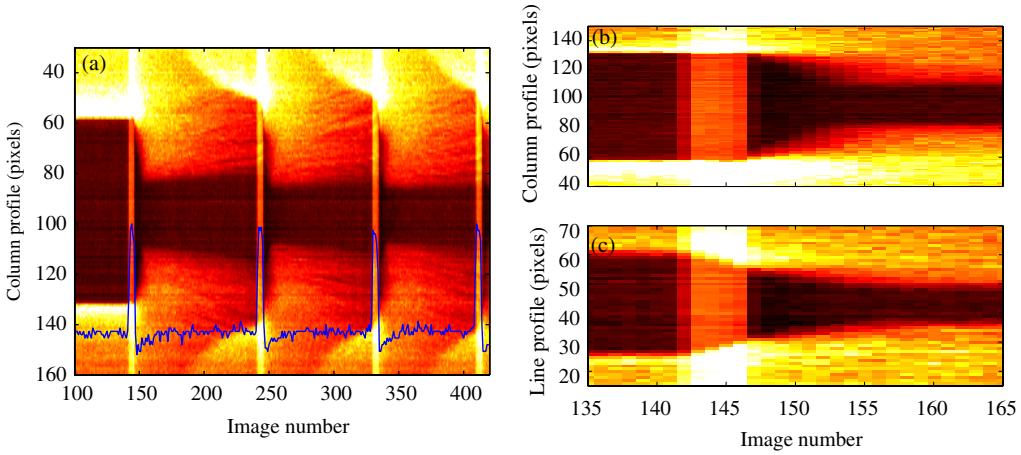

Figure 6. (a) Column profile (in false colours from dark red to bright yellow) calculated from image series presented in figure 5 with central plasma glow evolution superimposed (blue curve corresponding to line 95 of figure 6(a)), (b) zoom of (a), (c) corresponding line profile.

the characteristics of first and second contraction–expansion sequences are slightly different in terms of minimum void size and re-opening time duration. Concerning the time delay appearing in the vertical direction (as observed in figure 5) it can also be evidenced by comparing column and line profiles extracted from the video. These two profiles are shown respectively in figures 6(b) and (c). Previous results also showed that some correlation can be found between the different times of collapse and different slopes in electrical measurements [52]. Reasons why this effect appears in some cases are unclear due to a lack of statistics and spatiotemporal limitations of video acquisition. Nevertheless, one possible explanation is related to reactor geometry where confining conditions are different in the two directions. The electrode diameter is around 4 cm and glass boundaries are at approximately 3 cm of the electrode edges.

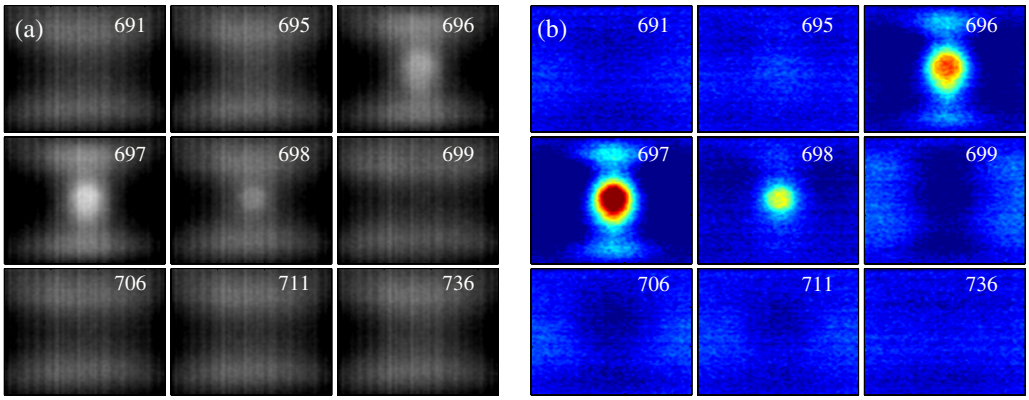

Figure 7. Heartbeat instability for a low repetition rate observed on the total plasma glow: (a) some images in true colours during one contraction–expansion sequence, (b) same images as in (a) with post-processing and false colours (from dark blue to red).

Consequently, the plasma usually extends beyond the electrodes towards the lateral sides. The plasma width is then nearly twice as large as the height and it is nearly the same for the trapped dust cloud and the void. No strong electrostatic barrier exists due to the distance to the glass boundaries, thus, plasma and void modifications in these directions are relatively free. On the contrary, the electrodes imposed a strong electrostatic barrier and vertical modifications and motions are then drastically controlled by the sheaths.

4. Plasma glow behaviour in the whole discharge

Plasma glow in the whole interelectrode volume is recorded during the instability in the two different cases (low and high repetition rate). This analysis is performed in order to understand global evolution of the plasma and not only central part behaviour as in the previous section. It can identify some side effects already suggested (relation between a sharp peak in electrical measurements and brighter glow regions near plasma horizontal boundaries [49, 51]) and that are inaccessible through the analysis presented in section 3.

4.1. Sequences with a low repetition rate

The total plasma glow recorded by fast imaging during a contraction–expansion sequence is shown in figure 7(a). Both bright presheath regions are clearly evidenced on the upper and lower parts of the images (electrodes are not visible). Before the contraction–expansion sequence (stable situation with an open void), the central plasma region is relatively uniform and not very bright (image 691). Then, the glow increases fast and concentrates in the discharge centre before disappearing and leaving a darker region in the centre as observed in the previous section. This scheme is better evidenced by representing the same images in false colours and by subtracting a reference image (stable situation) as shown in figure 7(b). The relatively homogeneous glow (image 691) changes into a bright (i.e. higher ionisation) central region and dark (i.e. lower ionisation) edges during the contraction (image 697). A reverse situation (dark centre and bright

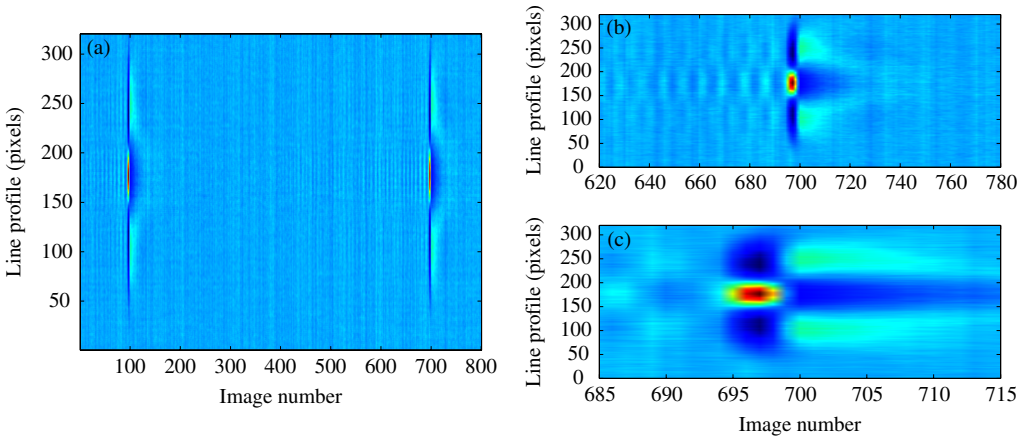

Figure 8. (a) Line profile (in false colours from dark blue to red) calculated from the image series presented in figure 7; (b) and (c) are different magnifications of (a).

edges) starts just before the re-opening (image 699). Then, the glow becomes slowly uniform again (image 736).

Time evolution of a line profile is presented in figure 8(a) and magnified in figures 8(b) and (c). To construct this false colour image, the horizontal line passing through the middle of the discharge is extracted from each video image. This line has been chosen because it passes through the region of biggest changes. In order to extract changes occurring during the instability, a temporal average value is subtracted. A smoothing filter is also applied for noise reduction and better delimitation of changing regions. Column profiling has also been performed for the plasma glow analysis but no original information has been extracted partly due to the limiting conditions imposed by electrodes.

Nearly isolated contraction–expansion sequences often have a short time duration. Figure 8 shows an instability frequency of about 3 Hz. In between each sequence, original conditions have time to be restored. From figures 8(b) and (c), plasma glow behaviour is well observed and its complete evolution analysis is more easily performed than from direct images like in figure 7. First, some small oscillations are observed before the real sequence. This phenomenon has already been observed [51, 52] and corresponds to failed contractions appearing sometimes near the instability existence threshold. This behaviour does not change the following analysis and will be described in a future article. Figure 8 confirms that when the void contracts, the plasma glow suddenly concentrates in the centre leaving dark border regions. The void re-opening occurs during the reverse situation with two symmetrical bright regions surrounding the plasma centre. Then, these regions seem to diffuse slowly to the centre until a homogeneous glow is obtained once again.

In the previous section, only the central part of the plasma was observed when the interference filter was removed. Indeed, the observed region was too small and due to the viewing angle, out of focal plane information was lost. The whole plasma recording allows to identify the dark (during contraction) and bright (during expansion) plasma edge regions. These observations show that the increase of plasma glow in the centre is really a concentration of the plasma towards the centre at the expense of the plasma edges. After that, the reverse situation occurs with plasma edges brighter than in the stable void situation.

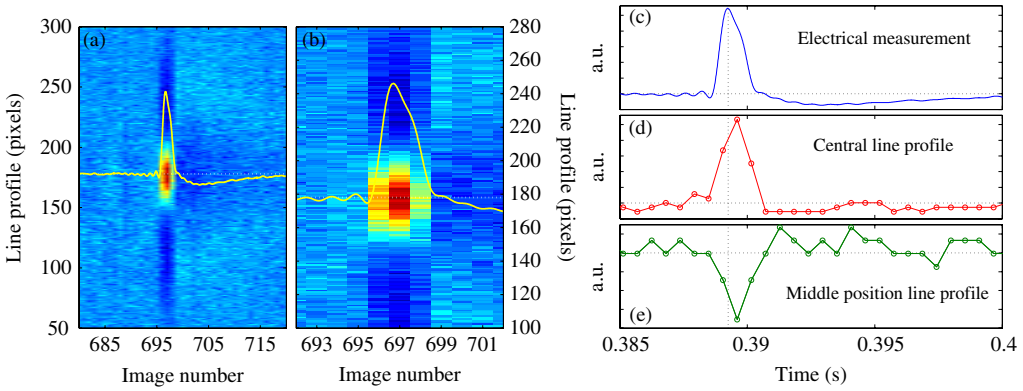

Figure 9. (a) Line profile (in false colours from dark blue to red) calculated from the image series presented in figure 7 with electrical measurements superimposed; (b) zoom of (a); (c) electrical measurements; (d) central line (line 178) profile of (a); (e) middle position line (line 105) profile of (a).

Correlation with electrical results is presented in figures 9(a) and (b) with non smoothed images in order to get pixel precision. The dotted curve is the current continuous component. From this superimposition it can be deduced that the contraction corresponds to an increase in the global ionisation (i.e. electron density). Indeed, increase of central plasma glow corresponds to an increase of electrical signal amplitude meaning that this central increase is not compensated by the decrease in the near plasma edge. Then, when the reverse situation occurs, ionisation appears to be below the stable situation value (as indicated by electrical measurements). Indeed, the dark central region is not balanced by the larger but slightly brighter near edge regions. Finally, these regions tend to rejoin in the centre following the slow increase observed in electrical measurements. These behaviours are also visible by comparing electrical measurements with line profiles (figures 9(c)–(e)) extracted from figure 9(a) (not to be confused with temporal evolution of line profile extracted from video images) and physically corresponding to the time evolution of individual pixels taken in (d) plasma centre and in (e) the near edge.

4.2. Sequences with a high repetition rate

When the heartbeat instability frequency increases, contraction–expansion sequences are closer in time, and no exact return to original stable conditions is achieved. Indeed, the next sequence happens while the void size has not reached its stable state. The case presented here is quite similar to the one shown in figures 5 and 6. The corresponding video is presented in figure 10 showing three successive contraction–expansion sequences. Images extracted from one sequence appear in figure 10(a). Figure 10(b) is obtained from figure 10(a) in the same way as figure 7(b). As the sequence lasts longer, better time resolution is obtained and variation of plasma glow is well evidenced. In comparison with the low repetition rate case, the change from bright centre and dark edges to the reverse is here more strongly marked. The different phases of the contraction–expansion sequence that have been already described, are highly visible here.

The deduced line profile is very significant and summarises nearly all results concerning plasma glow evolution during the heartbeat instability (figure 11). Indeed, starting from a void

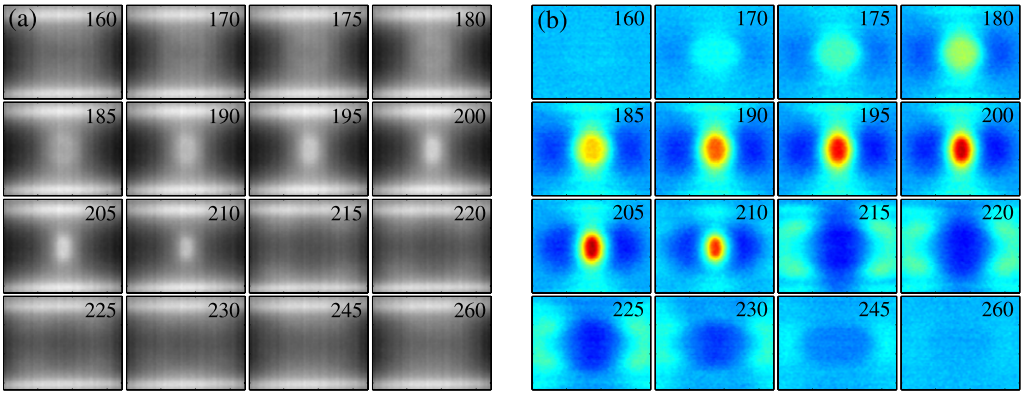

Figure 10. Heartbeat instability for a high repetition rate observed on the total plasma glow: (a) some images in true colours during one contraction–expansion sequence; (b) same images as in (a) with post-processing and false colours (from dark blue to red) (see also movie 4, 2.7 MB).

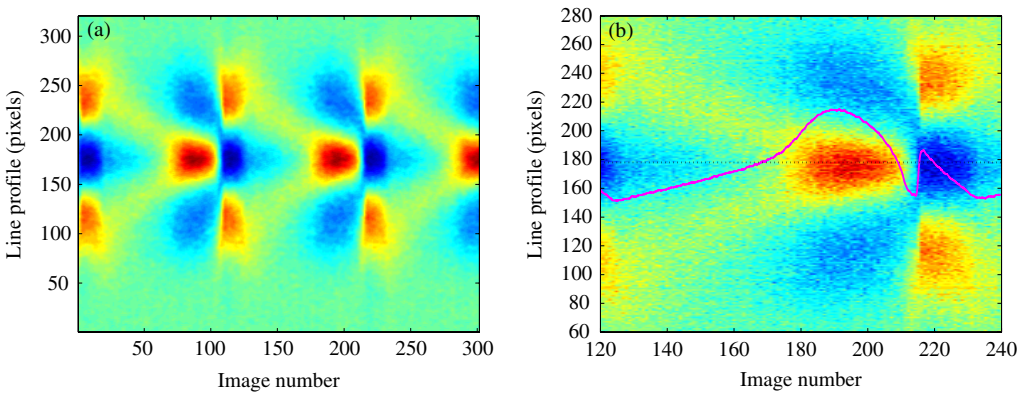

Figure 11. (a) Line profile (in false colours from dark blue to red) calculated from image series presented in figure 10; (b) zoom of (a) with electrical measurements superimposed.

expansion (dark inner part and bright plasma edges), slow concentration of the glow from the plasma edge towards the centre takes place. This motion can be correlated to the grey corona region observed in the dust cloud and presented in section 3. Furthermore, it clearly appears that the two brighter edge regions do not meet completely and no homogeneous plasma is restored as in figure 8. Indeed, the central glow increases at the expense of plasma edges before the brighter glow regions fully converge towards the plasma centre. This central enhancement is then followed by a strong and fast reversal. Electrical measurements are superimposed on the line profile in figure 11(b). The bright region moving from the plasma edge towards the plasma centre corresponds to a continuous increase of the current. Then, it appears that the strong brightness reversal is related to the presence of a sharp peak in the current. Measurements without peak certainly correspond to cases where the brightness reversal between plasma centre and edges exists, but is not strongly marked (figure 9). This sharp peak is an interesting feature already observed but not fully explained. Indeed, in [49], preliminary results suggested that this peak could be correlated to a strong glow decrease in the centre and increase in the

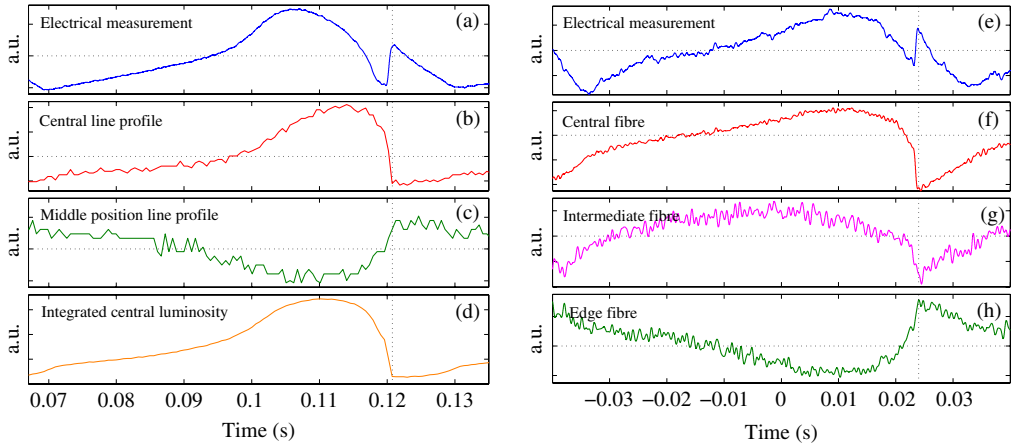

Figure 12. Extracted data from figure 11: (a) electrical measurements; (b) central line profile; (c) line profile in the glow reversal region. (d) Plasma glow integrated on a small central volume from complete image series of figure 10. Previous measurements in similar conditions for (e) electrical measurements; (f) light recorded by a centred optical fibre; (g) intermediate fibre; (h) edge fibre (same observed region as (c)).

plasma edge. These measurements were performed thanks to a spatially resolved (four different positions) analysis of an argon line emission at 750.4 nm. Further results with five optical fibres (also used for characterisation of dust particle growth instabilities [53]) and integrating all plasma wavelengths gave similar results [51] but no complete description was available. Present results greatly enhance spatiotemporal resolution of this phenomenon and clearly correlate the sharp peak with an enhancement of the plasma glow outside the central region. Variations of electrical measurements are representative of global changes of the plasma (spatially integrated measurement). From the present analysis it appears that electrical measurements are not only dominated by the plasma core.

These effects are also evidenced in figure 12 by direct comparison of (a) electrical measurements, with data extracted from figure 11: (b) central line profile (i.e. physically corresponding to central pixel variation), (c) middle position line profile (i.e. variation of a pixel in the glow reversal zone) and from the video in figure 10: (d) integrated central luminosity (i.e. variation integrated in a small centred volume assumed to represent plasma core). Comparison of figure 12(a), (b) and (d) shows that the main central plasma changes are observed in electrical measurements. Nevertheless, it appears that the maximum value of central glow occurs while electrical measurements have already decreased. In fact, at this time, electrical measurements are affected by the edge plasma glow decrease as observed in figure 12(c). Finally, the sharp peak region is well understood thanks to figure 11(b) and figure 12(a)–(d). Opposite behaviour of electrical measurements and central glow is directly related to the strong and fast enhancement of plasma edges while the centre becomes the less luminous part.

In order to show consistency of the new results, previous measurements performed in similar instability conditions (i.e. similar electrical measurements) with the optical fibre diagnostics, are presented in figure 12(e)–(h). Here, the edge fibre (figure 12(h)) observes the region corresponding to the middle line profile of figure 12(c). The intermediate fibre observes

a region in between the centre and the edge. Its maximum value appearing before the one of figure 12(f) traduces the plasma concentration towards centre. Main features concerning the sharp peak region are observed: the peak corresponds to a glow reversal between the centre and the edge. This comparison is of major interest because it confirms that no artefacts, neither in the way measurements are performed nor in data retrieval from images, are implied for explanation of the sharp peak region.

5. Discussion and conclusion

From the different analyses, several features of the heartbeat instability can be brought to the fore: the void contraction corresponds to an increase of the central plasma glow. These observations tend to show that a sudden higher ionisation in the plasma centre enhances the ratio between the inward electrostatic force and the outward ion drag force. Then, the void centre becomes darker but dust particles continue to move towards the centre due to their inertia. Their motion seems more or less continuous (at relatively constant speed) and is stopped suddenly (see for example figure 1). The void is not entirely filled by dust particles meaning that a force prevents further motion towards its centre. This force also exceeds gravity that should induce void collapse by acting on, among others, dust particles constituting the upper part of the void. At this time the central glow is not very bright. Furthermore, it appears more or less homogeneous, a property usually associated with a weak electric field. The force stopping dust particles is then supposed to be the ion drag.

Dust particles located near the plasma centre are then nearly immobile while a dust particle 'wave front' coming from the plasma edge starts to be detected. At this time, a corona region of higher ionisation is observed in plasma glow images. This region surrounds the plasma centre and moves slowly towards it. Correlating dust cloud images with plasma glow ones, this moving region seems to correspond to the dust particle wave front. Darker centre and brighter edge can create an outward electrostatic force near the corona region. This hypothesis is assumed by analogy with the contraction phase when an enhanced glow region attracts dust particles. Thus, central dust particles are immobile (far from this interface) and the wave front corresponds to dust particles close to the corona region and moving towards it. As dust particles move, local conditions change and the corona region moves towards the centre attracting inner dust particles one after the other. As the plasma becomes more and more homogeneous, the wave front speed decreases and the last dust particles to move are finally the closest to the plasma centre.

In the case of low repetition rate sequences, the original stable position of the void is restored between each sequence that can be considered as isolated and independent. On the contrary, high repetition rate conditions lead to a continuous motion of the dust particles. Indeed, while central dust particles return to their original position, a new contraction occurs.

An asymmetry in void contraction has been evidenced in some cases. This behaviour can find its origin in the discharge geometry, confined by electrodes in the vertical direction and more free to diffuse in the horizontal one. It is confirmed by the observed corona region in plasma glow images. Indeed, it is better observed near the horizontal edges than near the vertical ones where it is merged with the bright presheath regions.

The sharp peak in electrical measurements can be associated with the glow reversal from bright centre and dark edges to bright edges and dark centre. It appears when this phenomenon is strongly marked. It is replaced by a change in signal slope in other cases. This reversal is very fast and our camera system does not allow to resolve this phenomenon in time. The optical

fibre diagnostics have a high time resolution but noise is relatively important and the data do not show if there is a wave propagation between centre to edge during the reversal. The reversal seems to be instantaneous and its physical origin is under investigation.

Acknowledgments

The PKE-Nefedov chamber has been made available by the Max-Planck-Institute for Extraterrestrial Physics, Germany, under the funding of DLR/BMBF under grants No. 50WM9852. We would like to thank S Dozias for electronic support and J Mathias for optical support. ESA and Kayser-Threde GmbH are acknowledged for providing the high speed camera system in the framework of the IMPACT programme. This work was supported by CNES under contract 02/CNES/4800000059.

References

[1] Walch B, Horanyi M and Robertson S 1994 *IEEE Trans. Plasma Sci.* **22** 97
[2] Melzer A, Trottenberg T and Piel A 1994 *Phys. Lett.* A **191** 301
[3] Arnas C, Mikikian M and Doveil F 1999 *Phys. Rev.* E **60** 7420
[4] Samarian A A and Vladimirov S V 2003 *Phys. Rev.* E **67** 066404
[5] Ratynskaia S *et al* 2004 *Phys. Rev. Lett.* **93** 085001
[6] Couëdel L, Mikikian M, Boufendi L and Samarian A A 2006 *Phys. Rev.* E **74** 026403
[7] Morfill G E, Thomas H M, Konopka U, Rothermel H, Zuzic M, Ivlev A and Goree J 1999 *Phys. Rev. Lett.* **83** 1598
[8] Nefedov A P *et al* 2003 *New J. Phys.* **5** 33
[9] Roth R M, Spears K G, Stein G D and Wong G 1985 *Appl. Phys. Lett.* **46** 253
[10] Watanabe Y, Shiratani M, Kubo Y, Ogawa I and Ogi S 1988 *Appl. Phys. Lett.* **53** 1263
[11] Bouchoule A, Plain A, Boufendi L, Blondeau J P and Laure C 1991 *J. Appl. Phys.* **70** 1991
[12] Howling A, Hollenstein C and Paris P J 1991 *Appl. Phys. Lett.* **59** 1409
[13] Bouchoule A, Boufendi L, Hermann J, Plain A, Hbid T, Kroesen G, Stoffels E and Stoffels W W 1996 *Pure Appl. Chem.* **68** 1121
[14] Boufendi L, Gaudin J, Huet S, Viera G and Dudemaine M 2001 *Appl. Phys. Lett.* **79** 4301
[15] Cavarroc M, Jouanny M C, Radouane K, Mikikian M and Boufendi L 2006 *J. Appl. Phys.* **99** 064301
[16] Selwyn G S, Singh J and Bennett R S 1989 *J. Vac. Sci. Technol.* A **7** 2758
[17] Cavarroc M, Mikikian M, Perrier G and Boufendi L 2006 *Appl. Phys. Lett.* **89** 013107
[18] Roca i Cabarrocas P, Gay P and Hadjadj A 1996 *J. Vac. Sci. Technol.* A **14** 655
[19] Dutta A, Lee S P, Hayafune Y, Hatatani S and Oda S 2000 *Japan. J. Appl. Phys.* **39** 264
[20] Dutta A, Hayafune Y and Oda S 2000 *Japan. J. Appl. Phys.* **39** L855
[21] Deschenaux C, Affolter A, Magni D, Hollenstein C and Fayet P 1999 *J. Phys. D: Appl. Phys.* **32** 1876
[22] Hong S, Berndt J and Winter J 2003 *Plasma Sources Sci. Technol.* **12** 46
[23] Pereira J, Géraud-Grenier I, Massereau-Guilbaud V and Plain A 2005 *Thin Solid Films* **482** 226
[24] Stefanović I, Kovačevic E, Berndt J and Winter J 2003 *New J. Phys.* **5** 39
[25] De Bleecker K, Bogaerts A and Goedheer W 2006 *Phys. Rev.* E **73** 026405
[26] Robertson J 2002 *Mater. Sci. Eng.* R **37** 129
[27] Zhou D, McCauley T G, Qin L C, Krauss A R and Gruen D M 1998 *J. Appl. Phys.* **83** 540
[28] Szopa C, Cernogora G, Boufendi L, Correia J J and Coll P 2006 *Planet. Space Sci.* **54** 394
[29] Selwyn G S, McKillop J S, Haller K L and Wu J J 1990 *J. Vac. Sci. Technol.* A **8** 1726
[30] Ganguly B, Garscadden A, Williams J and Haaland P 1993 *J. Vac. Sci. Technol.* A **11** 1119
[31] Praburam G and Goree J 1996 *Phys. Plasmas* **3** 1212

[32] Mikikian M, Boufendi L, Bouchoule A, Thomas H M, Morfill G E, Nefedov A P, Fortov V E and PKE-Nefedov Team 2003 *New J. Phys.* **5** 19
[33] Winter J 1998 *Plasma Phys. Control. Fusion* **40** 1201
[34] Arnas C, Dominique C, Roubin P, Martin C, Brosset C and Pégourié B 2006 *J. Nucl. Mater.* **353** 80
[35] Dorier J L, Hollenstein C and Howling A 1995 *J. Vac. Sci. Technol.* A **13** 918
[36] Goree J, Morfill G E, Tsytovich V N and Vladimirov S V 1999 *Phys. Rev.* E **59** 7055
[37] Samsonov D and Goree J 1999 *Phys. Rev.* E **59** 1047
[38] Akdim M R and Goedheer W J 2001 *Phys. Rev.* E **65** 015401
[39] Jovanović D and Shukla P K 2003 *Phys. Lett.* A **308** 369
[40] Gozadinos G, Ivlev A V and Boeuf J P 2003 *New J. Phys.* **5** 32
[41] Avinash K, Bhattacharjee A and Hu S 2003 *Phys. Rev. Lett.* **90** 075001
[42] Tsytovich V N, Morfill G, Konopka U and Thomas H 2003 *New J. Phys.* **5** 66
[43] Zafiu C, Melzer A and Piel A 2003 *Phys. Plasmas* **10** 1278
[44] Schauer J C, Hong S and Winter J 2004 *Plasma Sources Sci. Technol.* **13** 636
[45] Kretschmer M, Khrapak S A, Zhdanov S K, Thomas H M, Morfill G E, Fortov V E, Lipaev A M, Molotkov V I, Ivanov A I and Turin M V 2005 *Phys. Rev.* E **71** 056401
[46] Vladimirov S V, Tsytovich V N and Morfill G E 2005 *Phys. Plasmas* **12** 052117
[47] Land V and Goedheer W J 2006 *New J. Phys.* **8** 8
[48] Goree J, Quinn R A, Morfill G E, Thomas H M, Hagl T, Konopka U, Rothermel H and Zuzic M 1998 *Proc. 4th Microgravity Fluid Physics and Transport Phenomena Conf.* (*Cleveland*)
[49] Mikikian M and Boufendi L 2004 *Phys. Plasmas* **11** 3733
[50] Mikikian M, Boufendi L and Bouchoule A 2003 *Proc. 30th EPS Conf. on Contr. Fusion and Plasma Phys.* (*St Petersburg*) (ECA vol 27A) ed R Koch and S Lebedev pp O–3.1B online at http://epsppd.epfl.ch/StPetersburg/pdf/O3_001b.pdf
[51] Mikikian M, Cavarroc M, Chaumeix N and Boufendi L 2004 *Proc. 31st EPS Conf. on Plasma Phys.* (*London*) (ECA vol 28G) ed P Norreys and H Hutchinson (Petit-Lancy: European Physical Society) pp O–2.13. Online at http://epsppd.epfl.ch/London/pdf/O2_13.pdf
[52] Mikikian M, Cavarroc M and Boufendi L 2005 *New Vistas in Dusty Plasmas* ed L Boufendi, M Mikikian and P K Shukla *AIP Conf. Proc.* vol 799 p 323
[53] Mikikian M, Cavarroc M, Couëdel L and Boufendi L 2006 *Phys. Plasmas* **13** 092103